Generalized transport-band field-effect mobility in disordered organic and inorganic semiconductors

P. Servati,[1] A. Nathan,[2] and G. A. J. Amaratunga[1]
[1]*Electrical Engineering Division, University of Cambridge, 9 JJ Thomson Avenue, Cambridge CB3 0FA, United Kingdom*
[2]*London Centre for Nanotechnology, University College London, London WC1H 0AH, United Kingdom*
(Received 25 April 2006; revised manuscript received 30 June 2006; published 15 December 2006)

Field-effect mobility μ_{FE} and its activation energy in disordered inorganic and organic semiconductor thin-film transistors is strongly dependent on bias conditions. This implies a nonlinear dependence of conductivity on carrier concentration, which stems from the high density of trapped carriers while only a few contribute to conduction. When μ_{FE} is extracted from measurement data, the nonlinear conductivity-concentration dependence is averaged over the semiconducting film. Consequently, μ_{FE} becomes mingled with device attributes such as gate capacitance in addition to terminal bias, which undermines the physical interpretation of μ_{FE} and subsequent comparison of measured values for different devices and different semiconductors. This paper presents an effective mobility μ_{eff} description at a reference carrier concentration, which separates the physical conductivity-concentration dependence from the device and bias attributes, enabling comparison of carrier transport in disordered semiconductors. In particular, by using the generalized concept of mobility edge and exponential band tails we show that μ_{eff} can be applied to a wide range of inorganic and organic semiconductors. Indeed, three parameters, viz., μ_{eff}, exponential band tail slope T_t, and bias-independent activation energy E_{a0} of μ_{eff}, can describe carrier transport in the transistor together with its bias and temperature dependence.

DOI: 10.1103/PhysRevB.74.245210 PACS number(s): 73.50.−h, 72.20.Ee, 73.61.Jc, 73.61.Ph

I. INTRODUCTION

Thin-film transistors (TFTs) using disordered inorganic and organic semiconductors have become attractive for emerging flexible electronics and active matrix organic light-emitting diode (AMOLED) displays.[1–7] For these transistors, parameters such as field-effect mobility μ_{FE} are primarily determined by disorder and grain size of the semiconductor, which in turn are strongly influenced by fabrication techniques (e.g., vacuum deposition, ink-jet printing, or spin coating) and the associated process conditions. In hydrogenated amorphous silicon (a-Si:H), the disorder in the bond lengths and angles leads to a high density of localized states. These states trap most of the electrons and the observed low conductivity can be attributed to the small fraction of carriers excited to the extended states.[8,9] In amorphous organic semiconductors, disorder in the molecular arrangement and the presence of grain boundaries lead to a high density of localized states.[1–3,10,11] Hopping of carriers between these states constitutes the means for conduction.

Despite differences in processes and presumed transport mechanisms in this family of materials, unique similarities are observed in the current-voltage (I-V) characteristics of the TFTs. The I-V characteristics generally follow a power-law dependence and the μ_{FE} is systematically bias dependent. For example, in a-Si:H TFTs, μ_{FE} gradually increases with increasing positive gate bias, which can be attributed to the increased number of electrons excited to extended states as the total density of accumulated electrons increases.[12–23] The same is observed for microcrystalline and nanocrystalline silicon TFTs.[24–27] Similarly, for a wide range of conjugated organic semiconductors, μ_{FE} increases with increasing negative gate bias (and hole accumulation).[10,11,28,29]

The dependence of μ_{FE} on carrier concentration is also reflected in the Arrhenius behavior of mobility in the temperature dependence measurements of a-Si:H and organic TFTs. Figure 1 illustrates temperature dependence of μ_{FE} for a-Si:H (our own), pentacene,[10] polythienylene vinylene (PTV),[10] and poly[5,5′-bis(3-alkyl-2-thienyl)-2,2′-bithiophene)] (PQT-12)[30,31] TFTs at different gate biases. Indeed the results for poly(3-hexylthiophene) (P3HT) TFTs, reported in Ref. 32, also falls close to PQT-12, which has been omitted for readability reasons. As seen, the mobility μ_{FE} generally shows Arrhenius behavior with an activation energy E_a, which decreases with increasing gate bias, as reported in literature.[10,18,20,21,30] The dependence of E_a on gate

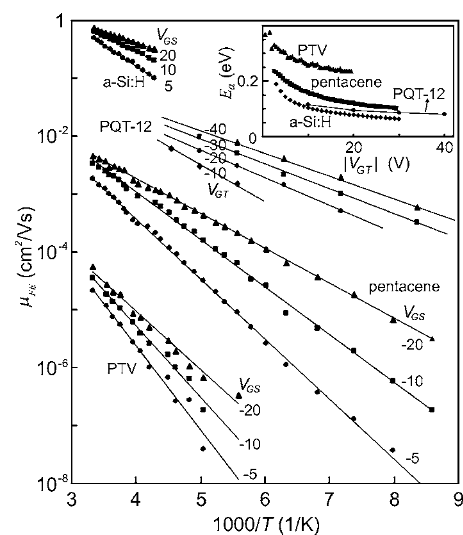

FIG. 1. Temperature dependence of reported values of μ_{FE} for a-Si:H, PQT-12 (Ref. 30), pentacene (Ref. 10), and PTV (Ref. 10) TFTs at different gate biases. The inset shows the bias dependence of activation energy E_a of μ_{FE} for these materials.

 ©2006 The American Physical Society

bias is solely due to the influence of carrier concentration on μ_{FE}.

The definition of the parameter μ_{FE} comes from planar transistors of crystalline semiconductors. In crystalline silicon field-effect transistors (FETs), mobility is scattering limited and its parasitic bias dependence is only due to surface or impurity scattering. Neglecting electron-electron interactions, carriers in crystalline silicon contribute to conduction independently, in which the conductivity σ is linearly dependent on the carrier density n, viz.,

$$\sigma = q\mu n. \tag{1}$$

Here, q is the elementary charge and μ the carrier mobility. The latter is determined by the relaxation time τ and the effective mass m^*. Measurements of conductivity in crystalline FETs provide information on field-effect mobility, since carrier concentration n is known and the relationship is linear.

Following the conventional linear field-effect mobility definition for a transistor, we have

$$\mu_{FE} = \frac{\partial g}{\partial Q}, \tag{2}$$

where g is the average conductance and Q is the average accumulated charge in the device. The field-effect mobility defined by Eq. (2) reduces to

$$\mu_{FE} = \frac{L}{WC_iV_{DS}}\frac{\partial I_{DS,lin}}{\partial V_{GS}}, \tag{3}$$

for the measured linear current $I_{DS,lin}$ (say V_{DS}=0.1 V) of a TFT, where W and L are the channel width and length, respectively, and V_{GS} and V_{DS} the gate-source and drain-source voltages, respectively. Often this is coupled with a capacitance-voltage measurement that determines the C_i term accurately.

When this parameter is used for disordered semiconductor FETs complexities arise. In the disordered material, σ is proportional to the density of carriers that contribute to conduction n_{band}, what we refer to as transport band carriers. However, most of the carriers are trapped and contribute in conduction only by excitation to the transport band. Consequently, Eq. (1) takes the form of $\sigma = q\mu n_{band}$ and the nonlinear relationship between n_{band} and the total carrier density n makes the extracted device mobility lose its true physical character. For a device under test, the conductance g as described in Eq. (2) is averaged over the semiconducting film and can be spatially related to the conductivity σ by

$$g^{-1} = \int_L \frac{dl}{\int_A \sigma da}, \tag{4}$$

where A is the cross section area and L the length of the semiconducting film. As seen from Eq. (4), g becomes a function of carrier density profile in the device. In addition, Q in the denominator of Eq. (2) comprises of trapped carriers and band carriers and similar to Eq. (4) should be integrated over the volume of the film. Consequently, μ_{FE} as principally defined by Eq. (2) varies with device parameters that include layer thicknesses (C_i) and bias conditions (V_{GS} and V_{DS}). In other words, the μ_{FE} as given by Eq. (2) and retrieved by Eq. (3) has a built-in dependence on carrier concentration n, and as such it is dependent on device geometry and bias for *a*-Si:H and organic TFTs.

Earlier works on *a*-Si:H (Refs. 12–23) use field-effect measurements coupled with numerical simulations and analytical methods to investigate the general characteristics of the density of states (DOS) in the bulk material. In particular, Shur *et al.*[13,14] have described the non-linear dependence of μ_{FE} on average induced charge Q in *a*-Si:H field-effect transistors at room temperature. However, a systematic description of the combined effect of temperature and gate bias on field-effect mobility along with the dependence of activation energy on bias will be invaluable. Indeed, a general description of mobility with bias and temperature dependence would enable a physically meaningful comparison of field-effect transport in both organic and inorganic semiconductors.

This paper exactly addresses these challenges. It revisits the conventional definition of μ_{FE} and presents it in the form $\mu_{FE} = \mu_{eff} \times \Theta$, where μ_{eff} is the physical mobility and Θ describes the device attributes. The dependence of μ_{eff} and Θ on bias and temperature must be explicitly analyzed to separate material properties from device dependent attributes. In the next section, we identify μ_{eff} based on an exponential density of tail states. Then, using $\Theta = \mu_{FE}/\mu_{eff}$ the discrepancy between the physical mobility and the conventional field effect mobility for different organic and inorganic semiconductors for a broad range of temperatures is presented. The activation energies of μ_{eff} and μ_{FE} as critical transport properties are then explicitly compared to identify the device dependent attributes. Finally, μ_{eff} is extended to represent hopping conduction and its temperature dependence in disordered organic semiconductors using the generalized concept of a transport band.

II. GENERALIZED TRANSPORT BAND WITH EXPONENTIAL TAIL

In disordered semiconductors, the DOS and transport mechanism are most critical for analysis of field-effect mobility μ_{FE}. These are functions of the material system and processing conditions. In the analysis presented here, we use a generalized transport band with an exponential band tail which constitute a good basis for electronic transport in these systems.[28,33] A mobility edge is often observed despite different transport mechanisms,[30] which makes the case for an isoelectronic transport band.

The density of carriers excited to the isoelectronic transport band n_{band}, in accordance to Boltzmann's approximation, can be written as

$$n_{band} = N_b \exp(E_F/kT), \tag{5}$$

where N_b is the effective state density for the transport band, k the Boltzmann's constant, T the temperature, and E_F the Fermi energy that is defined negative with respect to the mobility edge.

The density of trapped carriers can also be found from the density of localized states in the mobility gap. Often, an exponential DOS such as

$$g(E) = N_t / kT_t \exp(E/kT_t), \quad (6)$$

is used for the band tail, where E is the energy of the state and is defined negative with respect to the mobility edge. Here, N_t is the total number of tail states, and T_t the characteristic temperature indicating the width of the exponential distribution. Despite its simplicity, the exponential model of Eq. (6) can be generalized to represent a wide range of fast changing density of states. In the typical range of operating conditions, different distributions such as Gaussian can be effectively approximated by an equivalent exponential distribution.[34,35]

Based on the Fermi-Dirac distribution and as discussed in the Appendix, the density of trapped carriers takes the following general form:

$$n_{\text{trapped}} = N_t' \exp(E_F / kT_t'), \quad (7)$$

where N_t' is the density of trapped carriers at $E_F=0$ and T_t' the characteristic slope of the trapped carriers. The dependence of T_t' and N_t' on T_t and T is elaborated in the Appendix, in which we find that at relatively low temperatures ($T \ll T_t$), $T_t' \sim T_t$, and $N_t' \sim N_t$. By increasing the temperatures ($T \geq T_t/2$), T_t' slowly increases from its low temperature value T_t, which implies that low temperature measurements are required for accurate extraction of T_t.

Equations (5) and (7) show that both trapped and band carriers are exponentially dependent on E_F, however, with different activation energies. The smaller activation for band carriers leads to a relatively higher density of conducting carriers as carrier concentration increases. When the density of conducting carriers is averaged over the semiconducting layer, this leads to a bias dependence of μ_{FE}. However, as both densities change exponentially, by using Eqs. (5) and (7) one finds the density of band carriers in terms of the trapped carriers as

$$n_{\text{band}} = \frac{N_b}{(N_t')^{T_t'/T}} n_{\text{trapped}}^{T_t'/T}. \quad (8)$$

In addition, since $n_{\text{trapped}} \gg n_{\text{band}}$, the total carrier density $n = n_{\text{trapped}} + n_{\text{band}} \sim n_{\text{trapped}}$ can be replaced in Eq. (8) to yield

$$n_{\text{band}} = \theta n^{T_t'/T}, \quad (9)$$

where $\theta = N_b/(N_t')^{T_t'/T}$. This equation has been found to empirically hold for determining the equilibrium between free carrier density and total carrier concentration for a wide range of disordered semiconductors and operating conditions, including many organic semiconductors.[33] An exponentially increasing trapped and free carrier densities is the only assumption underlying Eq. (9), which holds for most disordered systems with fast changing DOS over a limited Fermi energy movement. In addition, to arrive at Eq. (7), we assume that the Fermi energy is above the deep states. This manifests as a threshold voltage adjustment and will be discussed later.

III. EFFECTIVE MOBILITY

The generality of Eq. (9) can be used to define an effective mobility that does not include device attributes. The density of carriers in the transport band as given by Eq. (9) determines conduction according to

$$\sigma = q \mu_{\text{band}} n_{\text{band}}. \quad (10)$$

The combination of Eqs. (9) and (10) shows a nonlinear relationship between conductivity and carrier density n. Here, we can summarize transport behavior in terms of the power term T_t'/T and the conductivity at a reference carrier concentration N_0. More explicitly, we define an effective mobility μ_{eff} at N_0 as

$$\mu_{\text{eff}} = \frac{\sigma|_{n=N_0}}{qN_0} = \mu_{\text{band}} \frac{N_b}{N_0} \left(\frac{N_0}{N_t'} \right)^{T_t'/T}. \quad (11)$$

Consequently, the conductivity-concentration relationship can be described by presenting μ_{eff} and T_t'/T according to

$$\sigma = q \mu_{\text{eff}} N_0 \times (n/N_0)^{T_t'/T}. \quad (12)$$

To show the significance of this representation, we will use it to obtain current-voltage characteristics of a TFT. Using the gradual channel approximation for the linear current $I_{\text{DS,lin}}$ we can write

$$I_{\text{DS,lin}} = \frac{W}{L} V_{\text{DS}} \int_0^{\delta} \sigma(y) dy, \quad (13)$$

where y denotes the location across the channel and δ is the channel depth. Using Eq. (12) for σ and changing the integral parameter from y to n, we find after mathematical manipulation[13,14,20,23]

$$I_{\text{DS,lin}} = \mu_{\text{eff}} \zeta \frac{W}{L} (C_i V_{\text{GT}})^{\alpha-1} V_{\text{DS}}, \quad (14)$$

where $V_{\text{GT}} = V_{\text{GS}} - V_T$, $\alpha = 2T_t'/T$ the power parameter in the saturation current-voltage characteristics, and

$$\zeta = \frac{(2\epsilon k T_t' N_0)^{1-\alpha/2}}{\alpha - 1}. \quad (15)$$

Here, ζ is just a function of T_t'/T and accounts for the carrier distribution across the film and ϵ the dielectric constant of the semiconductor layer. Comparing these findings to the definition of μ_{FE} in Eq. (3), we have

$$\mu_{\text{FE}} = \mu_{\text{eff}} \zeta (\alpha - 1)(C_i V_{\text{GT}})^{\alpha-2} \quad (16)$$

or

$$\Theta = \mu_{\text{FE}} / \mu_{\text{eff}} = \zeta (\alpha - 1)(C_i V_{\text{GT}})^{\alpha-2}, \quad (17)$$

which clearly represents the geometrical and bias attributes in μ_{FE}. Figure 2 illustrates Θ at room temperature in the linear regime as a function of T_t for different values of $C_i V_{\text{GT}}$. We observe an increasing discrepancy between μ_{FE} and μ_{eff} as T_t and $C_i V_{\text{GT}}$ increase. Note that Θ in Eq. (17) is strictly valid in the linear regime, which limits the use of the extracted μ_{FE} in other operating regimes. For example, using

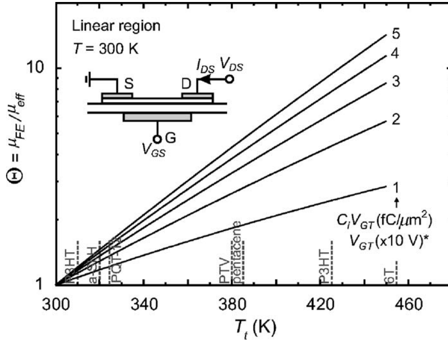

FIG. 2. $\Theta=\mu_{FE}/\mu_{eff}$ as a function of T_t for different C_iV_{GT} values, showing the impact of device parameters such as bias and geometry on the extracted mobility based on Eq. (3). The inset shows a cross section of a TFT. The ticks on T_t axis represent the reported positions for a-Si:H, PTV, pentacene, P3HT, and PTV as summarized in Table I. An asterisk denotes different values of V_{GT} for $C_i=10$ nF/cm^2 (the approximate capacitance of 500 nm silicon nitride).

μ_{FE} to predict the saturation current based on the conventional crystalline square-law dependence yields $\alpha(\alpha-1)/2$ times higher than expected current values. For $T_t=400$ K, this leads to an error of about a factor of 2 due to the discrepancy in the saturation charge distribution. This can also explain the observed disconnect between values of μ_{FE} extracted from linear and saturation regimes.

Representation of μ_{eff} and Θ based on Eqs. (11) and (17) is determined by T_t'/T, which is valid only when there is an exponential relationship between the carrier concentration and Fermi energy E_F as given by Eq. (7). This is true for a Fermi energy movement window that lies in the exponentially increasing tail states, much lower than the mobility edge and higher than the energies of the deep states. The Fermi energy must be no closer than a few kT_t' to the mobility edge to ensure the accuracy of Eq. (7), which generally holds due to the high density of tail states. This suggests that the value of N_0 should be selected from within this Fermi energy movement window below the mobility edge. In addition, since the deep states mostly contribute to the threshold voltage V_T and are filled before the device turns ON, the mobility definition of Eq. (11) is valid for the above-threshold regime. In other words, the reference concentration N_0 must be selected so that the Fermi energy E_{F0} associated with N_0 (see Fig. 3) resides well above the deep states. This requires that the charge accumulated in the channel $Q_{channel}$ to be higher than the charge C_iV_T needed to turn ON the device. Using Eq. (7) and Poisson's equation, $Q_{channel}=C_iV_0$ when the carrier concentration at the semiconductor interface is N_0, where $V_0=(2\epsilon kT_t'N_0)^{1/2}/C_i$. Consequently, to have $Q_{channel}>C_iV_T$, we must have $V_0>V_T$ or $N_0>C_i^2V_T^2/(2\epsilon kT_t')$, indicating the lower limit for selection of N_0. For $V_T=1-2$ V and $C_i=20$ nF/cm^2, which are typical values, we have $N_0>6\times10^{16}$ cm^{-3}. Assuming $N_0=10^{17}$ cm^{-3} to compare μ_{eff} values for different materials, we have $\zeta=(4.1\times10^{-16}\alpha)^{(1-\alpha/2)}/(\alpha-1)$. It is important to note that extraction of μ_{eff} and Θ from μ_{FE} relies on having an accurate value for α. This can be extracted from curvature of current-voltage characteristics[23] C-V methods or other physical methods.[36] Any error in the value of α (due to device nonidealities such as contact resistance) leads to an imperfect removal of the influence of device attributes from the field-effect mobility.

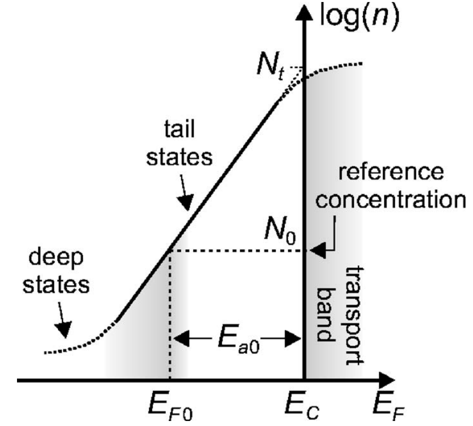

FIG. 3. Density of trapped carriers as a function of Fermi energy showing reference concentration and transport band.

The temperature dependence of μ_{FE} is commonly used to describe carrier transport in disordered semiconductors, and the activation energy E_a of μ_{FE} is found to be voltage dependent as well (see Fig. 3). We consider the temperature dependence of μ_{eff} by recasting Eq. (11) in the following manner:

$$\mu_{eff}=\mu_{eff0}\exp(-E_{a0}/kT), \tag{18}$$

where

$$\mu_{eff0}=\mu_{band}\frac{N_b}{N_0} \quad \text{and} \quad E_{a0}=kT_t'\ln\left(\frac{N_t'}{N_0}\right)=-E_{F0}. \tag{19}$$

This predicts Arrhenius behavior for the effective mobility with activation energy E_{a0}, which is given by the constant E_{F0}. Here, E_{F0} is the Fermi energy associated with the reference concentration N_0 as shown in Fig. 3 and represents the energy difference between transport mobility edge E_{band} and E_{F0}. In other words, the activation energy of μ_{eff} denotes the energy needed for carriers to thermalize from E_{F0} to the mobility edge and is bias independent. A closer look at the temperature dependence of μ_{FE} and μ_{eff} shows that

$$\frac{\partial\mu_{FE}}{\mu_{FE}\,\partial T}=\frac{\partial\mu_{eff}}{\mu_{eff}\,\partial T}+\frac{\partial\Theta}{\Theta\,\partial T}=-\frac{E_{a0}}{kT^2}+\frac{2T_t'}{T^2}\ln\left|\frac{V_{GT}}{V_0}\right|. \tag{20}$$

This clearly correlates the voltage dependence of activation energy of μ_{FE} to the temperature dependence of Θ. The conventional activation energy E_a for μ_{FE} may be written in terms of the bias-independent activation energy E_{a0} of μ_{eff} as

$$E_a(V_{GT})=E_{a0}-2kT_t'\ln|V_{GT}/V_0|, \tag{21}$$

which describes the voltage dependence observed in Arrhenius plots for μ_{FE}.[10] This description for bias dependence of activation energy holds for the range of temperatures and carrier concentrations where Eq. (9) holds and for a generalized transport band model.

IV. HOPPING TRANSPORT BAND

Hopping transport based on percolation or variable range hopping (VRH) is used to explain transport in organic semiconductors.[1,10,37] Despite different transport models for these materials, the mobility is found to be influenced by carrier concentration, resulting in temperature dependences similar to that of a-Si:H as shown in Fig. 1. This shows that the concept of effective mobility can be extended to these semiconductors so as to separate the material transport property from device and bias attributes. To develop an effective mobility description, a well-defined equilibrium between trapped and free carriers needs to be established. Evidence of this equilibrium, such as $n_{\text{band}}=\theta n^{T_t'/T}$ given in Eq. (9), in organic semiconductors has been reported[33] for a wide range of temperatures and carrier concentrations. For this relation to hold, the distribution of trapped and band carriers should be exponential. Although a Gaussian trap distribution is evident in organic materials,[34,38] for the typical range of operating conditions and Fermi energy movement window, the Gaussian distribution effectively reduces to an equivalent exponential distribution due to the small shifts in the Fermi energy.[35] For the density of band carriers, Grünewald *et al.*[39] and Shapiro *et al.*[40] have demonstrated the presence of a transport band in which hopping conduction dominates irrespective of the position of Fermi energy. Similar to the mobility edge, the trapped carriers are thermalized to this hopping band $E_{a0,\text{VRH}}$.[37] Relative to E_{F0}, the hopping band can be stated as

$$E_{a0,\text{VRH}} = kT_t' \ln\left[\frac{\gamma^3}{N_0}\left(\frac{2T}{3T_t'}\right)^3\right], \tag{22}$$

where γ is the effective overlap parameter for electronic states of the band tail. Baranovskii *et al.*[41,42] has generalized this concept of transport band beyond the exponential DOS assumption and to a broader range of disordered semiconductors with Gaussian or similar fast changing state. This concept can also accommodate the hopping transport based on percolation as described in Ref. 10 for amorphous organic semiconductors. Here, it can be shown that having a transport band at an energy corresponding to a carrier concentration of $N_t=B_C(2\gamma T/T_t')^3/\pi$, can replicate the same Arrhenius plots of μ_{FE}, where $B_C\sim 2.8$ is the critical number for percolation in three-dimensional amorphous systems. The position of the percolation hopping energy band is just $kT_t'\ln(B_C/3\pi^3)\sim -3.5kT_t'$ away from that is predicted by Monroe's VRH.[37] Table I summarizes the values for μ_{eff} at room temperature T_t' and E_{a0}, at $N_0=10^{17}$ cm^{-3} determined from the results presented for different disordered systems in the literature.

V. CONCLUSIONS

The quest for new inorganic and organic semiconductor materials has challenged the interpretation of basic carrier transport properties such as field-effect mobility. The mobility in these complex material systems is systematically dependent on device geometry and terminal bias due to the nonlinear influence of carrier concentration on conductivity, thus undermining the crystalline and planar-transistor definition of mobility. This paper presents an effective mobility description that separates device attributes from the physical mobility to facilitate a direct comparison of mobility in a variety of disordered material systems. The activation energy of the effective mobility is independent of bias and denotes the energy needed for carriers to thermallize to the transport band, providing a consistent physical interpretation of the carrier transport. Using generalized transport band definition, this mobility description can be extended to hopping transport in organic semiconductors and provides means for tabular comparison of device properties.

TABLE I. Extracted values of transport parameters (μ_{eff}, T_t, and E_{a0}) from published data for disordered semiconductors such as a-Si:H, pentacene, PTV, P3HT, PQT-12, sexithiophene (6T), dihexyl-sexithiophene (DH6T), and poly(phynelene vynelene) (PPV) at $N_0=10^{17}$ cm^{-3}.

Semiconductor	μ_{eff} @ 300 K (cm^2/Vs)	T_t (K)	E_{a0} (eV)	Ref.
a-Si:H	0.8	320	0.230	23
pentacene	9.0×10^{-4}	385	0.313	10
PTV	1.1×10^{-5}	380	0.418	10
P3HT	5.5×10^{-5}	425		34 and 43
P3HT	0.060	310	0.293	32
PQT-12	0.034	324	0.245	30
6T	1.6×10^{-3}	455	0.313	28
DH6T	0.010	495	0.260	28
PPV	5×10^{-6}	540	0.450	44

ACKNOWLEDGMENTS

P.S. and A.N. would like to acknowledge the financial support of Natural Sciences and Engineering Research Council (NSERC) of Canada.

APPENDIX

The density of trapped carriers as a function of Fermi energy is retrieved from the density of states $g(E)$ using

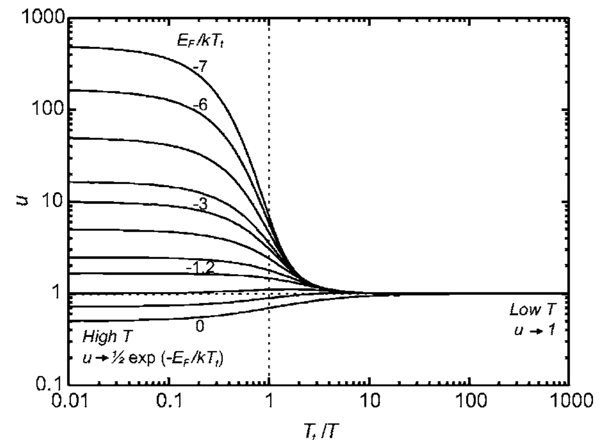

FIG. 4. Simulation results for u in Eq. (A3) as a function of T_t/T and E_F.

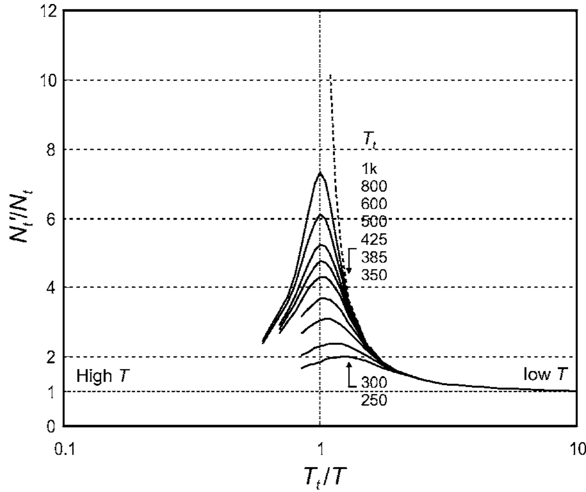

FIG. 5. N_t' as a function of T_t/T. Dashed lines show the frequently used Eq. (A5) and its deviation from simulation results.

$$n_{\text{trapped}} = \int_{E_G}^{0} g(E) f(E,E_F) dE, \tag{A1}$$

where $f(E,E_F)$ denotes the Fermi-Dirac function

$$f(E,E_F) = \{1 + \exp[(E - E_F)/kT]\}^{-1}, \tag{A2}$$

and E_G the bandgap. For an exponential density of states such as Eq. (6), we find after mathematical manipulation[13,14,23]

$$n_{\text{trapped}} = N_t \exp(E_F/kT_t) u, \tag{A3}$$

where

$$u(E_F,T_t,T) = \int_{x_{GF}}^{x_F} \frac{dx}{1 + x^{T_t/T}},$$

and $x_F = \exp(-E_F/kT_t)$ and $x_{GF} = \exp[(E_G - E_F)/kT_t]$ are the boundaries for the integral parameter x. Based on numerical simulations as shown in Fig. 4, the integral u on the right hand side of Eq. (A3) approaches unity at low T

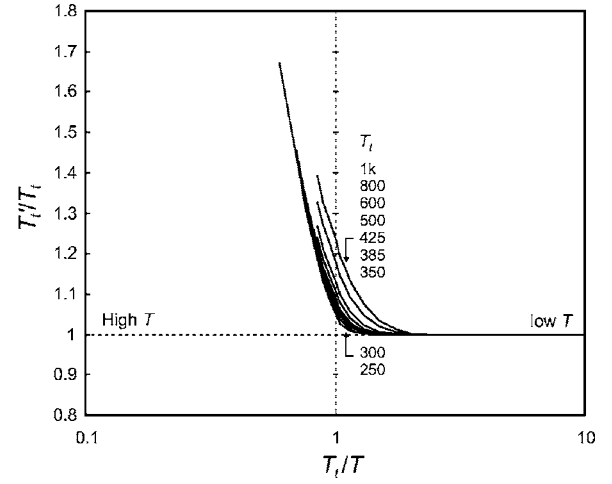

FIG. 6. T_t' as a function of T_t/T.

$(T \ll T_t)$, simplifying the result to $n_{\text{trapped}} = N_t \exp(E_F/kT_t)$. In contrast, at high T $(T \gg T_t)$, $u \to 1/2 \exp(-E_F/kT_t)$, resulting in $n_{\text{trapped}} \to N_t/2$. For intermediate temperatures $(T_t/10 < T < 10T_t)$, u attains a value between these two extremes. Although this integral is not analytically solvable over all temperatures, one finds that n_{trapped} as a function of E_F has a general exponential characteristic in typical temperature ranges, and thus can be written as

$$n_{\text{trapped}} = N_t' \exp(E_F/kT_t'), \tag{A4}$$

where N_t' and T_t' are the magnitude and slope of the exponential and are functions of T and T_t. Figures 5 and 6 depict the dependence of N_t' and T_t' on T_t and T. At low T, $T_t' \sim T_t$ and

$$N_t'/N_t \sim \frac{\sin(\pi T/T_t)}{\pi T/T_t}, \tag{A5}$$

which is often used by different authors.[4,13,14] However, as T increases and becomes comparable to T_t $(T > T_t/2)$, the characteristic slope T_t' increases and is more influenced by T or thermal energy. In addition, N_t' shows bell shaped behavior and deviates from the popular expression of Eq. (A5).

[1] R. A. Street, Nat. Mater. **5**, 171 (2006).
[2] H. Sirringhaus *et al.*, Nature (London) **401**, 685 (1999).
[3] S. R. Forrest, Nature (London) **428**, 911 (2004).
[4] M. Matters, D. M. de Leeuw, M. J. C. M. Vissenberg, C. M. Hart, P. T. Herwig, T. Geuns, C. M. J. Musaers, and C. J. Drury, Opt. Mater. **12**, 189 (1999).
[5] A. Nathan, A. Kumar, K. Sakariya, P. Servati, S. Sambandan, and D. Striakhilev, IEEE J. Solid-State Circuits **39**, 1477 (2004).
[6] G. Li, J. Shinar, and G. Jabbour, Phys. Rev. B **71**, 235211 (2005).
[7] P. Servati and A. Nathan, Proc. IEEE **93**, 1257 (2005).
[8] M. H. Cohen, H. Fritzsche, and S. R. Ovshinsky, Phys. Rev. Lett. **22**, 1065 (1969).
[9] W. E. Spear and P. G. Le Comber, J. Non-Cryst. Solids **8-10**, 739 (1972).
[10] M. C. J. M. Vissenberg and M. Matters, Phys. Rev. B **57**, 12964 (1998).
[11] R. A. Street, J. E. Northrup, and A. Salleo, Phys. Rev. B **71**, 165202 (2005).
[12] A. Nagy, M. Hundhausen, L. Ley, G. Brunst, and E. Holzenkämpfer, Phys. Rev. B **52**, 11 289 (1995).
[13] M. Shur, M. Hack, and J. G. Shaw, J. Appl. Phys. **66**, 3371 (1989).
[14] M. Shur and M. Hack, J. Appl. Phys. **55**, 3831 (1984).
[15] A. Madan, P. G. Le Comber, and W. E. Spear, J. Non-Cryst. Solids **20**, 239 (1976).
[16] M. J. Powell and J. W. Orton, Appl. Phys. Lett. **45**, 171 (1984).
[17] V. Augelli, V. Berardi, R. Murri, L. Schiavulli, M. Leo, R. A. Leo, and G. Soliani, Phys. Rev. B **35**, 614 (1987).

[18] N. B. Goodman and H. Fritzsche, Philos. Mag. B **45**, 407 (1982).
[19] M. J. Powell, Philos. Mag. B **43**, 93 (1981).
[20] R. L. Weisfield and D. A. Anderson, Philos. Mag. B **44**, 83 (1981).
[21] R. E. I. Schropp, J. Snijder, and J. F. Verwey, J. Appl. Phys. **60**, 643 (1986).
[22] M. J. Powell, C. van Berkel, A. R. Franklin, S. C. Deane, and W. I. Milne, Phys. Rev. B **45**, 4160 (1992).
[23] P. Servati and A. Nathan, IEEE Trans. Electron Devices **50**, 2227 (2003).
[24] T. Dylla, F. Finger, and E. A. Schiff, Appl. Phys. Lett. **87**, 032103 (2005).
[25] C. H. Lee, A. Sazonov, and A. Nathan, Appl. Phys. Lett. **86**, 222106 (2005).
[26] I. C. Cheng, S. Allen, and S. Wagner, J. Non-Cryst. Solids **338**, 720 (2004).
[27] J. Puigdollers, C. Voz, A. Orpella, I. Martín, D. Soler, M. Fonrodona, J. Bertomeu, J. Andreu, and R. Alcubilla, J. Non-Cryst. Solids **299-302**, 400 (2002).
[28] G. Horowitz, R. Hajlaoui, and P. Delannoy, J. Phys. III **5**, 355 (1995).
[29] C. D. Dimitrakopoulos, S. Purushothaman, J. Kymissis, A. Callegari, and J. M. Shaw, Science **283**, 822 (1999).
[30] A. Salleo, T. W. Chen, A. R. Völkel, Y. Wu, P. Liu, B. S. Ong, and R. A. Street, Phys. Rev. B **70**, 115311 (2004).
[31] B. S. Ong, Y. Wu, P. Liu, and S. Gardner, J. Am. Chem. Soc. **126**, 3378 (2004).
[32] B. H. Hamadani and D. Natelson, Proc. IEEE **93**, 1306 (2005).
[33] A. J. Campbell, M. S. Weaver, D. G. Lidzey, and D. D. C. Bradley, J. Appl. Phys. **84**, 6737 (1998).
[34] C. Tanase, E. J. Meijer, P. W. M. Blom, and D. M. de Leeuw, Org. Electron. **4**, 33 (2003).
[35] D. Natali and M. Sampietro, J. Appl. Phys. **92**, 5310 (2002).
[36] C.-Y. Huang, S. Guha, and S. J. Hudgens, Phys. Rev. B **27**, 7460 (1983).
[37] D. Monroe, Phys. Rev. Lett. **54**, 146 (1985).
[38] M. Gailberger and H. Bässler, Phys. Rev. B **44**, 8643 (1991).
[39] M. Grünewald, B. Movaghar, B. Pohlmann, and D. Würtz, Phys. Rev. B **32**, 8191 (1985).
[40] F. R. Shapiro and D. Adler, J. Non-Cryst. Solids **74**, 189 (1985).
[41] S. D. Baranovskii, T. Faber, F. Hensel, and P. Thomas, J. Phys.: Condens. Matter **9**, 2699 (1997).
[42] S. D. Baranovskii, O. Rubel, and P. Thomas, Thin Solid Films **487**, 2 (2005).
[43] E. J. Meijer, C. Tanase, P. W. M. Blom, E. van Veenendaal, B. Huisman, D. M. de Leeuw, and T. M. Klapwijk, Appl. Phys. Lett. **80**, 3838 (2002).
[44] C. Tanase, E. J. Meijer, P. W. M. Blom, and D. M. de Leeuw, Phys. Rev. Lett. **91**, 216601 (2003).